Current Biology, Volume *27*

Supplemental Information

ADF/Cofilin Accelerates Actin Dynamics by Severing Filaments and Promoting Their Depolymerization at Both Ends

Hugo Wioland, Berengere Guichard, Yosuke Senju, Sarah Myram, Pekka Lappalainen, Antoine Jégou, and Guillaume Romet-Lemonne

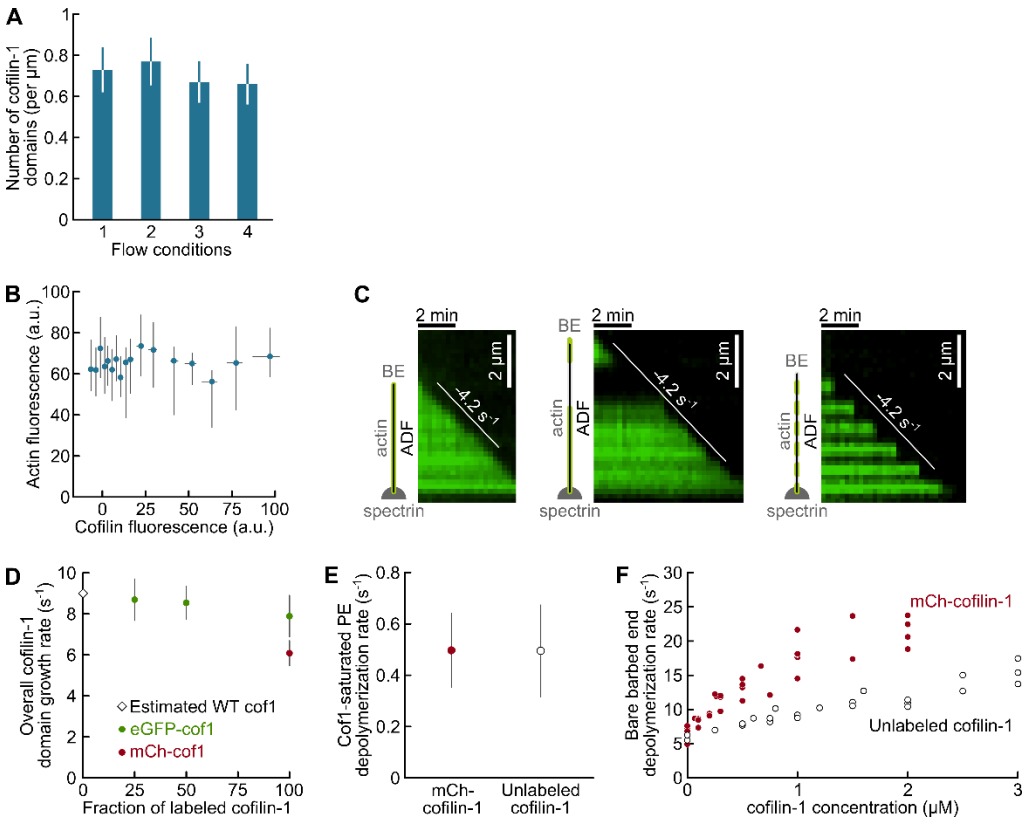

Figure S1. Control experiments: flow conditions and fluorescent labeling do not affect the measured rates (related to STAR Methods, and figures 1-4).

(A) Alexa488-labeled ADP-actin filaments were exposed to 200 nM mCherry-cofilin-1 for 18 seconds, under different flow conditions, and cofilin-1 domains were then counted. For each experiment, N=30-40 domains, on 5 different filaments, each 9-12 µm long. Error bars represent standard deviations. Flow conditions while exposing to mCherry-cofilin-1 : (1) constant 30 mbar for 18 seconds; (2) 30 mbar for 2 sec, 6 mbar for 14 sec, 30 mbar for 2 sec; (3) 6 mbar for 18 sec; (4) 30 mbar for 2 sec, 0 mbar for 14 sec, 30 mbar for 2 sec. The indicated pressures are the pressure in the reservoir of the cofilin-1 solution. The local flow rate scales with this pressure [S1].
(B-C) Actin labelling does not affect actin and ADF/cofilin dynamics. (B) Cofilin-1 binding is not affected by the local actin labeling density. Alexa488-actin filaments were exposed for 15 s to 0.4 µM mCh-cofilin-1. The actin (before exposure to cofilin) and cofilin fluorescent signals were measured (mean over 5 pixels across the filament and normalized by the background fluorescence). Each circle represents the median over 30 data point (error bars: interquartile range). (C) ADF-saturated labeled filaments depolymerize as fast as unlabeled ones. To estimate the depolymerization rate of unlabeled actin, we generated a long segment (middle panel) or multiple short segments (right panel) of unlabeled actin, within filaments labeled with Alexa488 (at our standard labeling fraction of 15%). Filaments were all saturated with ADF and depolymerization was carried out with 0.5 µM ADF in solution.

(D-F) Effect of fluorescent labeling on cofilin binding and cofilin-induced depolymerization (related to Figures 1, 3 and 4). Fluorescent cofilin was required for some of our experiments, and we then used N-terminal mCherry- and eGFP-fusions of cofilin-1 and cofilin-2. In these experiments, we estimated the impact of labeling by varying the fraction of labeled cofilin we used (D). In other experiments, where labeling was not required to measure its effect, we compared our results using 0% or 100% labeling (E-F).
(D) Growth rate of cofilin-1 domains on unlabeled cytoplasmic ADP-actin. Cofilin-1 concentration was kept constant at 350 nM, changing only the labeling fractions. A high mCherry labeling fraction moderately reduced the growth rate of cofilin domains, while labeling with eGFP has no significant effect. Data points are mean ± SD (N = 11 to 19). Diamond symbol: estimated growth rate of a fully unlabeled cofilin-1 domain, computed assuming labeled and unlabeled cofilin-1 bind independently, each with its own on-rate. In the manuscript, we used eGFP-cofilin (not mCherry-cofilin) to estimate binding constants (Figure 1).
(E) Pointed end depolymerization of cofilin-1-saturated filaments is unaffected by cofilin-1 labelling. Data points are mean ± SD (N = 186 from 10 experiments for mCherry-cofilin-1, and N = 32 for unlabeled cofilin-1). In the

manuscript, the depolymerization rates of saturated filaments were determined using unlabeled ADF/cofilin (Figures 4 and 5).

(F) Labelling of cofilin-1 enhances its impact on the barbed end of bare filaments. In the manuscript, the depolymerization rates of bare barbed ends were determined using unlabeled ADF/cofilin (Figure 3).

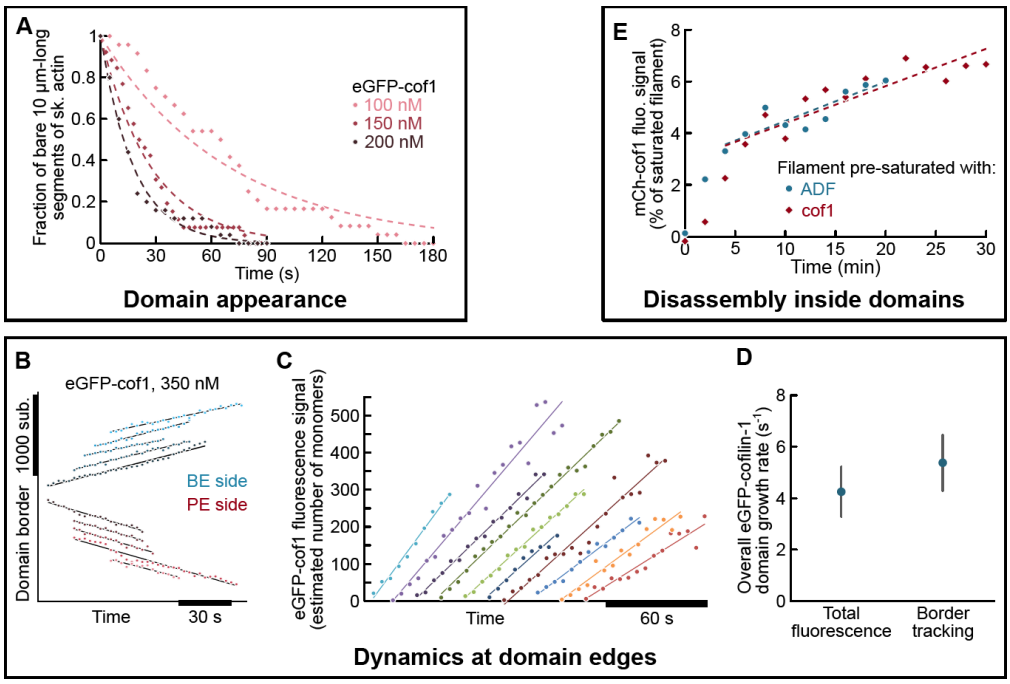

Figure S2. Methods to measure ADF/cofilin domain assembly dynamics (related to figure 1).

(A) Domain appearance rate. Fraction of a population of 10-µm-long unlabeled skeletal actin segments which bear no detectable eGFP-cofilin-1 domain, decreasing over time during exposure to various concentrations of cofilin-1. Dotted lines are exponential fits, yielding the domain appearance rate (shown in Figure 1E).

(B-D) Assembly and disassembly at cofilin domain edges. We used two methods to measure domain growth rates. The first is to track the borders of domains as they grow over several pixels (B). This method allows to compare the growth towards the BE versus PE (Figure 1F) but it requires domains to appear sparsely in order to have enough space to grow to significant sizes. In particular, it could not be used for high cofilin concentrations on skeletal actin, because the domain density rapidly became too high. An alternative method is to measure the increase in total fluorescence of one growing domain over time (C), normalized by that of a single fluorophore (determined from fully saturated filaments). This allowed us to measure the growth rate of very small domains. Here, we compare the two methods.
(B) Growth of eGFP-cofilin-1 (350 nM) domains on unlabelled cytoplasmic actin. The position of individual domain edges were tracked over time (data points). Lines are linear fits yielding the growth rate.
(C) Fluorescent signal over time, for 10 eGFP-cofilin-2 domains. The time origin is offset, for clarity. Lines: linear fits. Each data point corresponds to the fluorescence of a 6 by 3 to 4 pixels region, from which the background fluorescence has been subtracted.
(D) Comparison between the two methods on the same movie (150 nM eGFP-cofilin-2 on unlabeled cytoplasmic actin). Total fluorescence: average over the 10 fits in (C). Border tracking: sum of the growth towards the PE (averaged over 19 borders) and the BE (averaged over 9 borders). Error bars: standard deviation.

(E) ADF/cofilin disassembly from within a domain. As shown in Figure 1 H-I, filaments were saturated with unlabelled ADF or cofilin-1 before exposing to mCherry-cofilin-1. We here quantify the increase of the overall mCherry-cofilin-1 fluorescence signal normalized by that of a saturated filament, over time. Data points represent the mean values over 7 filaments. Dotted lines are linear fits (approximating an exponential) yielding “koff,inside”. To minimize sensitivity to the background value (substracted from the data) the first points, with the lowest intensity, are left out of the fit. The resulting values are in Figure 1J.

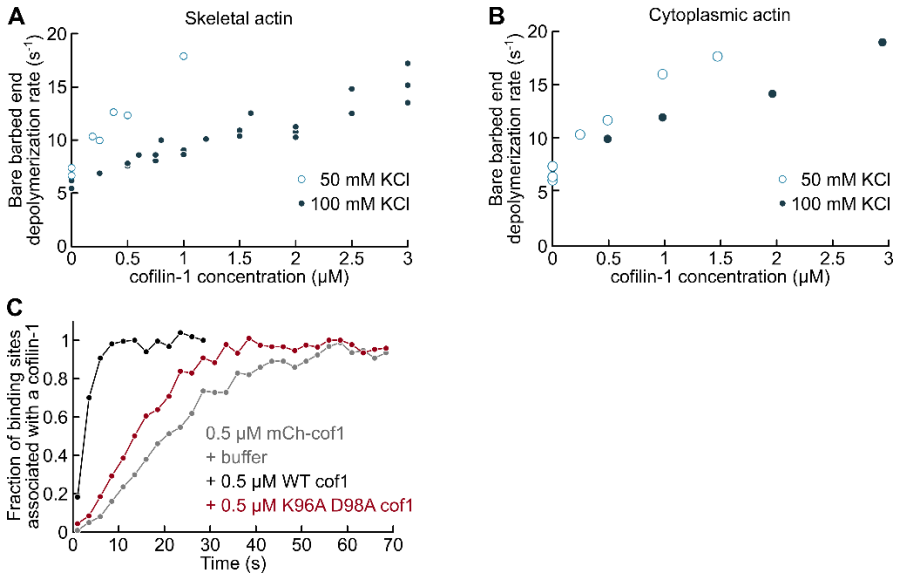

Figure S3. Depolymerization at bare barbed-ends (related to Figure 3).

(A-B) Effect of salt on the depolymerization rate of bare filament barbed ends exposed to cofilin-1. Skeletal (A) and cytoplasmic (B) ADP-actin, labeled with 15% Alexa488, was exposed to mCherry-cofilin-1 (A) or unlabeled cofilin-1 (B,C). Open symbols: 50 mM KCl, full symbols: 100 mM KCl. Each data point is the median over 18 to 55 filaments. Using a higher salt concentration limits the formation of ADF/cofilin domains thus allowing us to measure the depolymerization of bare BE over a larger range of concentrations. We used 100 mM KCl only in our experiments shown in Figures 3C and 3D.

(C) Mutations K96A D98A on the F-site of cofilin-1 hinders its binding to skeletal actin filaments. The K96A D98A cofilin-1 mutant is unlabeled. To compare its binding rate to that of WT cofilin-1, the total fluorescent signal of WT mCherry-cofilin-1 normalized by that of fully saturated filaments is plotted over time, for 3 different conditions: 0.5 µM mCherry-cofilin-1 (grey), 0.5 µM mCherry-cofilin-1 + 0.5 µM unlabeled cofilin-1 (black) and 0.5 µM mCherry-cofilin-1 + 0.5 µM unlabeled K96A D98A cofilin-1 (red). N=10 filaments for each condition. The mutant shows an intermediate behavior: while it is still able to bind F-actin, its affinity is about 4-fold lower than WT-cofilin-1. Actin filaments were 15% labeled with Alexa-488.

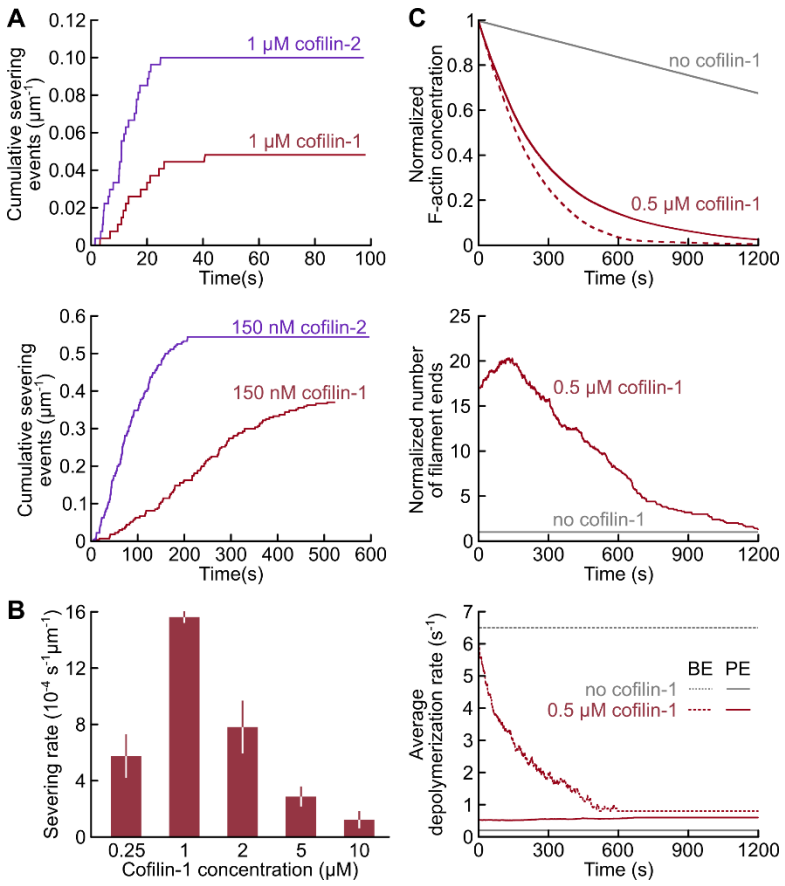

Figure S4. Global outputs, computed by numerical simulations integrating individual reaction rate constants (related to Figures 1-4).

(A) Cumulative severing over time, for filaments exposed to 1 µM and 150 nM of cofilin-1 and cofilin-2 (comparable to Fig 2b and 2e of Chin et al. [S2]). Each curve was computed for a population of 20 filaments, each initially 13.5 µm long.

(B) Severing rate for different cofilin-1 concentrations (comparable to Fig 1B of Nadkarni and Brieher [S3]). For each concentration, the severing rate was computed over the first 30 seconds, for 3 populations of 20 filaments, each initially 13.5 µm long. Error bars represent standard deviations.

(C) Top: depolymerization of 2.5 µM ADP-F-actin over time, by sequestration of G-actin at t=0, following 5 minutes of incubation (not shown) with 0.5 µM cofilin-1 (red) or buffer (gray). Each simulation corresponds to an initial population of 10 filaments, each 67.5 µm long. The dashed red line takes pyrene quenching into account (comparable to Fig. 4C of Kremneva et al. [S4]). Middle: for the same set of simulated filaments, evolution of the number of ends over time. At t=0 in the presence of cofilin-1 the number of ends has been increased more than 15-fold by the severing events which occurred during the 5 minutes of incubation (before t=0). Bottom: for the same set of simulated filaments, evolution of the average depolymerization rates for BE and PE. Over time, as filaments get saturated by cofilin-1, the global depolymerization rate of pointed ends increases mildly and does not compensate the slowing down of barbed end depolymerization. Here, the cofilin-1-induced enhancement of filament disassembly is due to the demultiplication of depolymerizing ends by severing.

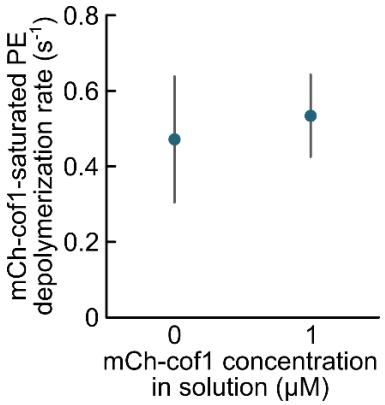

Figure S5. Pointed end depolymerization is not affected by cofilin-1 in solution (related to Figures 4 and 5). Depolymerization rate at PE of mCherry-cofilin-1-saturated skeletal actin filaments. The presence of mCherry-cofilin-1 in solution does not affect the depolymerization rate. Mean values over 6 and 4 experiments, with a total of N = 102 and 84 filaments, for 0 and 1 µM cofilin-1, respectively.

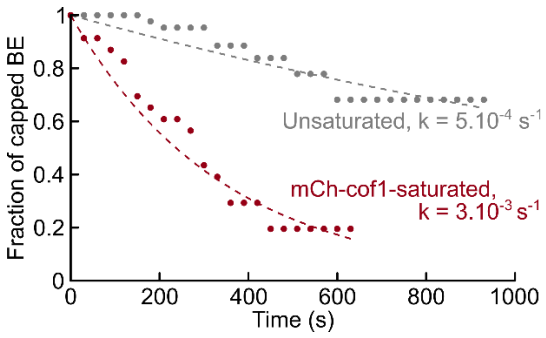

Figure S6. Cofilin1-saturated filaments are uncapped faster than bare filaments (related to Figure 5D)
The departure of CP was measured on bare filaments (grey) and on mCherry-cofilin-1-saturated filaments (red). This is equivalent to the data shown for ADF-saturated filaments in Figure 5D. However, due to the slower depolymerization of cofilin-1-saturated barbed ends, the transition from pause (capped state) to depolymerization (uncapped) was more difficult to pinpoint. In our analysis, any unclear state was considered as a pause, so that the CP off-rate we determined here for cofilin-1-saturated is an underestimate of the actual value.

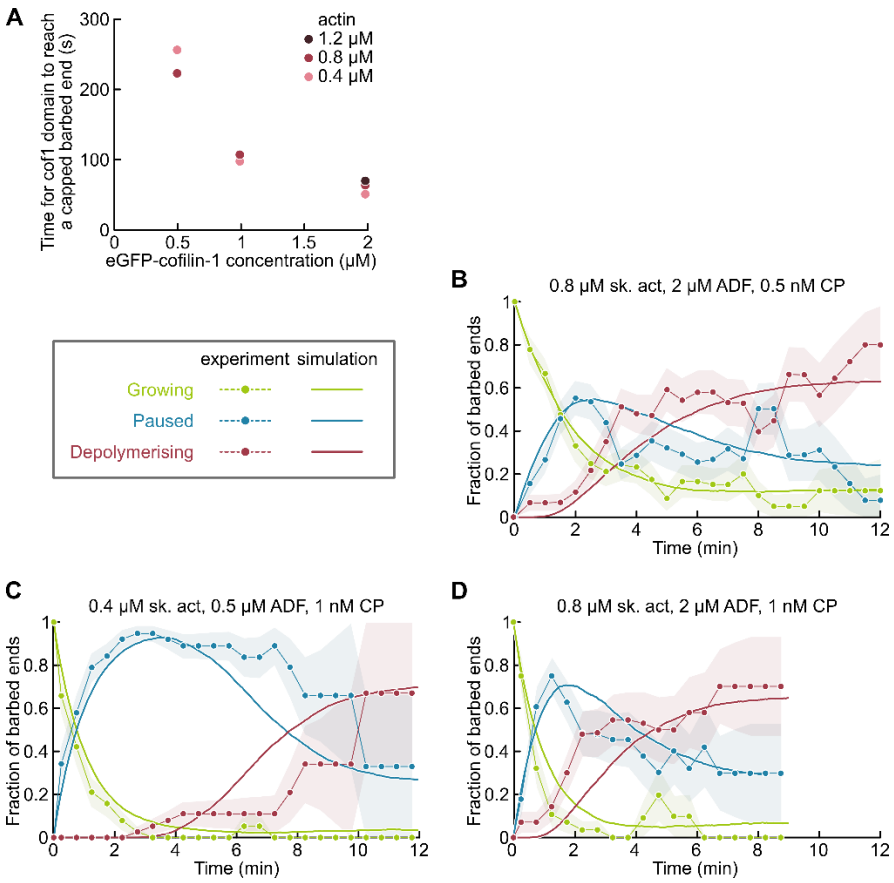

Figure S7. Synergy between ADF/cofilin and CP generates depolymerizing BE under different conditions (related to Figure 6).

(A) Once the BE is capped, the ADF/cofilin domains can fully saturate the filament (Figure 6D). To estimate the time for an ADF/cofilin domain to reach the capped BE, we measured the mean length of the bare actin segment near the BE for growing filaments (ADP-Pi cap, Figure 3G) in the presence of different concentrations of Alexa594-ATP-G-actin and eGFP-cofilin-1. Over time, this bare segment length fluctuated around a constant value, i.e. the average growth of the domain towards the BE equaled the average elongation rate of the filament. The time to reach the capped BE is then calculated as this length divided by the elongation rate of the filament (N = 7 – 10 filaments).

(B-D) Fractions of BE growing, paused and depolymerizing in the presence of 0.4 to 0.8 μM Alexa488-ATP-G-actin, 0.5 to 2 μM ADF and 0.5 to 1 nM CP. Symbols indicate fractions calculated from experiments, excluding severing events, for populations of N=45 (B), 38 (C) and 28 (D) filaments. Full lines are non-fitted simulations based on reaction rates calculated independently.

SUPPLEMENTAL REFERENCES

S1. Jégou, A., Niedermayer, T., Orbán, J., Didry, D., Lipowsky, R., Carlier, M.F., and Romet-Lemonne, G. (2011). Individual actin filaments in a microfluidic flow reveal the mechanism of ATP hydrolysis and give insight into the properties of profilin. PLoS Biol. *9,* e1001161.

S2. Chin, S.M., Jansen, S., and Goode, B.L. (2016). TIRF microscopy analysis of human Cof1, Cof2, and ADF effects on actin filament severing and turnover. J. Mol. Biol. *428*, 1604–1616.

S3. Nadkarni, A. V., and Brieher, W.M. (2014). Aip1 destabilizes cofilin-saturated actin filaments by severing and accelerating monomer dissociation from ends. Curr. Biol. *24*, 2749–2757.

S4. Kremneva, E., Makkonen, M.H., Skwarek-Maruszewska, A., Gateva, G., Michelot, A., Dominguez, R., and Lappalainen, P. (2014). Cofilin-2 controls actin filament length in muscle sarcomeres. Dev. Cell *31*, 215–226..